Clinical Neurophysiology 130 (2019) 379–387

Contents lists available at ScienceDirect

Clinical Neurophysiology

journal homepage: www.elsevier.com/locate/clinph

Scotopic multifocal visual evoked potentials

D.S. Muranyi [a,b], F.H. Kramer [a,c], A. Herbik [a], M.B. Hoffmann [a,d,*]

[a] Department of Ophthalmology, Otto-von-Guericke University Magdeburg, Germany
[b] Department of Ophthalmology, Martin-Luther University Halle, Germany
[c] Beuth University of Applied Sciences, Berlin, Germany
[d] Center for Behavioral Brain Sciences, Magdeburg, Germany

ARTICLE INFO

Article history:
Accepted 27 November 2018
Available online 31 December 2018

Keywords:
mfVEP
Scotopic
Latency
Visual field test
Human
Visual cortex

HIGHLIGHTS

- Photopic multifocal visual evoked potentials (mfVEP) yield objective visual field testing.
- Scotopic mfVEPs are pioneered and important insights are provided.
- Scotopic mfVEPs may hold promise for an objective visual field test.

ABSTRACT

Objective: To investigate the scope of scotopic multifocal visual evoked potentials ($mfVEP_S$) for the assessment of scotopic visual fields.
Methods: Pattern-reversal mfVEP for photopic ($mfVEP_P$) and scotopic conditions ($mfVEP_S$; 0.003 cd/m^2) were recorded from 36 visual field locations of a circular checkerboard pattern (25° radius) in 9 participants with normal vision. $MfVEP_P$ were recorded with a conventional central fixation cross, $mfVEP_S$ were recorded (i) with ($mfVEP_{S+}$) and (ii) without ($mfVEP_{S-}$) an additional fixation aid. Latency shifts were determined using cross-correlations, mfVEP magnitudes were analysed in an eccentricity dependent manner using signal-to-noise ratios (SNRs).
Results: In comparison to $mfVEP_P$, $mfVEP_{S-}$ and $mfVEP_{S+}$ were delayed by 101 ms and 97 ms, respectively, and had smaller signal-to-noise-ratios. Both $mfVEP_S$ were reduced down to noise level in the center and also severely reduced for the most peripheral stimulus eccentricity used. The visual-field-coverage for the paracentral eccentricities of $mfVEP_{S+}$ and $mfVEP_{S-}$ was 76% and 65% [4°–9°], respectively, and 79% and 66% [9°–16°].
Conclusions: $MfVEP_S$ were delayed compared to $mfVEP_P$ and demonstrated the expected central response drop-out typical for scotopic vision.
Significance: $MfVEP_S$ may hold promise of an objective, spatially resolved visual field test which motivates testing it in patients with diseases affecting scotopic vision.

1. Introduction

Non-invasive electrophysiology is an important tool for the objective assessment of visual function in humans, which allows tapping different stages of the visual pathways (Bach and Kellner, 2000; Heckenlively and Arden, 2006). Retinal recordings with the electroretinogram (ERG) are used to investigate retinal function, cortical recordings with visual evoked potentials (VEP) are used to investigate the integrity of the visual pathway in its entirety. Both techniques can be combined with the multifocal technique, an approach to record responses from multiple visual field locations within a short time frame (Sutter, 1985, 1991, 2000). Consequently, multifocal ERGs (mfERGs) and multifocal VEPs (mfVEP) enable us to assess the visual field topography of retinal and cortical function, respectively. MfVEP allow for an assessment of visual pathway integrity and for objective visual field testing (Hood and Greenstein, 2003; Hoffmann, 2008; Hoffmann and Flechner, 2008; Hoffmann et al., 2003, 2006, 2011, 2015, 2018). Consequently, they are a valuable tool to resolve cases of unexplained visual field defects. Importantly, current applications of mfVEP-based objective visual field testing are confined to photopic testing

* Corresponding author at: Universitäts-Augenklinik, Visual Processing Laboratory, Leipziger Str. 44, 39120 Magdeburg, Germany.
E-mail address: michael.hoffmann@med.ovgu.de (M.B. Hoffmann).

https://doi.org/10.1016/j.clinph.2018.11.030
1388-2457/

conditions, yet the scope of objective visual field testing with scotopic mfVEP has not been probed.

Scotopic vision is mediated by the rod system and has a number of distinct characteristics (Zele and Cao, 2014). Specifically, due to the rod-free fovea (Curcio et al., 1990), scotopic vision is associated with a central scotoma (Aulhorn and Michelfelder, 1972; Barton and Brewer, 2015; Baseler et al., 2002; Hadjikhani and Tootell, 2000; Hubel et al., 2009). Furthermore, under scotopic conditions the signal is strongly delayed compared to photopic processing (MacLeod, 1972; Markó et al., 2012). While these features impact on the recording conditions, they also serve as identifiers of truly scotopic signals. Based on previous studies pioneering scotopic mfERGs (Hood et al., 1998; Chen et al., 2004; Feigl et al., 2005, 2006), we here aimed to establish a framework for scotopic mfVEP recordings. We compared photopic and scotopic mfVEP, i.e. $mfVEP_P$ and $mfVEP_S$, to test for the scotopic latency delay and central response dropout, i.e. typical hallmarks of scotopic vision.

2. Methods

2.1. Participants

Nine participants (median age: 27; range: 23–36 years; 4 females; 5 male) took part in two experiments. All participants had a best corrected decimal visual acuity of ≥1.0 as tested with FrACT (Bach and Kellner, 2000; Heckenlively and Arden, 2006). The participants gave their written consent prior to the study. The procedures followed the tenets of the declaration of Helsinki and the protocol was approved by the ethics committee of the University of Magdeburg, Germany.

2.2. Procedure

Our procedures were in general accordance with our previous studies [e.g. (Herbik et al., 2014)] as indicated below, with adaptations of the approach to our specific study aim as detailed below. In the present study a series of two experiments were conducted in separate sessions on different days; each session had a total duration of 2 h. In each of the two experiments two blocks of $mfVEP_P$ were recorded followed, after 30 min of dark adaptation, by two blocks of $mfVEP_S$. As detailed below, in Experiment 1 a conventional fixation cross was presented for both $mfVEP_P$ and $mfVEP_{S-}$ recordings, in Experiment 2 an additional fixation aid in the stimulus center was presented for $mfVEP_{S+}$. Four participants started with Experiment 1, the remaining five participants with Experiment 2. In both experiments, the participants viewed, supported by a chin rest, the stimuli monocularly (right eye) at 33 cm distance wearing the optimal refractive correction. In accordance with current VEP standards (Odom et al., 2016) the participants' pupils were not dilated to maximize retinal image quality. No extreme pupil sizes or anisochoria were observed.

2.3. Stimulation

VERIS 6.4.7X (EDI: Electro-Diagnostic Imaging, San Mateo, CA, USA) was used for stimulus delivery and electrophysiological recordings. The stimuli were presented on a monochrome monitor (MDG403, Philips; P45 phosphor) driven with a frame rate of 75 Hz. The visual stimulus with a white fixation cross spanning the entire display was presented on a grey background (Fig. 1A). For the photopic conditions, i.e. for $mfVEP_P$ recordings, the mean

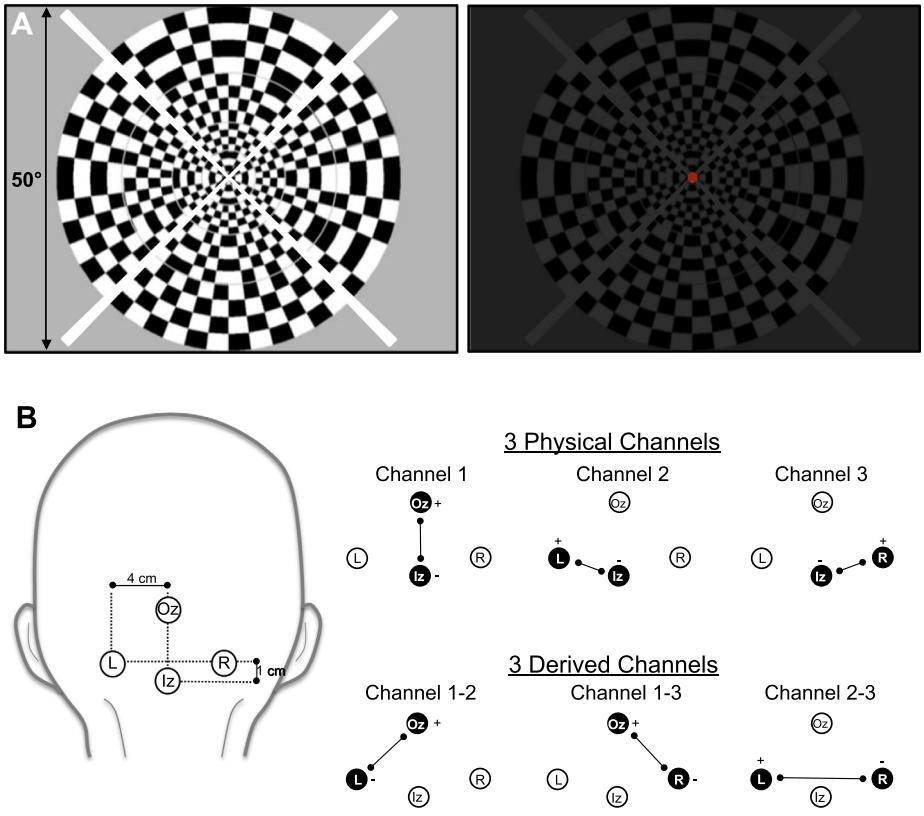

Fig. 1. (A) Dartboard pattern with 36 patches, comprising 4 different eccentricity ranges (indicated by gray circles), and a white fixation cross used for multifocal visual evoked potential recordings for photopic ($mfVEP_P$, left panel) and scotopic stimulation with a dimmed central red ($mfVEP_{S+}$; right panel as depicted) or without ($mfVEP_{S-}$). (B) Recording sites for the mfVEP recordings. Position of recording electrodes on back of the head of a participant as detailed in Methods (left panel) and the three physical channels referenced to the inion (Iz) and the three recording sites obtained after re-referencing the physical channels (right panels).

luminance (CS-100A photometer; Konica Minolta Holdings, Inc.; Japan) was set to 103 cd/m^2 (stimulus and gray background) with a contrast of 96%. For the scotopic conditions, i.e. for mfVEP$_S$ recordings, luminance settings were reduced by a factor of 32,000 with a neutral-density filter [Haida Optical Glass 150Series; ND 4.5 (32,000×), product number 7014, Haida Photo Supplies Co., Ningbo, China] down to a mean luminance of 0.003 cd/m^2. In Experiment 2 the same stimulus was presented, except for an additional fixation aid, a centrally placed dimmed (luminance: 0.245 cd/m^2) red diode (Lumitronix 3 mm LED, 11000mcd, red, Product number 13602) during the scotopic condition (Fig. 1A).

2.4. Stimulus pattern and sequence

"The stimulus pattern, a circular dartboard (diameter 50°) depicted in Fig. 1, was subdivided into 36 individual fields, each comprising a checkerboard of 4 × 4 checks, such that mfVEP were recorded from 36 separate visual field locations with independent pattern-reversal stimuli. The elements were arranged in 4 rings spanning following eccentricity ranges: 0°–4°, 4°–9°, 9°–16°, 16°–25°. The temporal and spatial independence of the stimulation sequences is essential for the multifocal technique. This is achieved by the use of binary m-sequences ["maximum length sequences" (Cohn and Lempel, 1977)], which have practical advantages that are due to the property that a different starting point in an m-sequence cycle results in a mathematically independent, i.e. orthogonal, m-sequence. Therefore, the same m-sequence can be applied for each visual field location, as long as different starting points are guaranteed. Consequently, independent stimulation in the individual patterns followed a binary m-sequence (Sutter, 1991). It consisted of a pseudo-random succession of 0 and 1 states," (Herbik et al., 2014) with a 50% chance for each state and step. An m-sequence length of $2^{14} - 1$, i.e. 16383, steps was used. For the pattern-reversal stimulation applied in the present study these two states were the two contrast-inverted states of each checkerboard field. Importantly, each state lasted 3 frames (39 ms) to account for the delayed scotopic responses and the decreased scotopic flicker fusion frequency. For a frame duration of 39 ms, a pattern reversal occurs on average every 78 ms, resulting in 12.8 reversals per second, which is above the scotopic flicker fusion frequency of approximately 15 Hz (Hecht and Shlaer, 1936). The recordings were subdivided into 16 overlapping segments each lasting about 39 s to allow the participants to blink and to alleviate steady fixation during the actual recordings. A single recording block for each condition took around 11 min. Each condition was presented twice (2× mfVEP$_P$, 30 min dark adaption, 2× mfVEP$_S$) resulting in a total session duration (including preparation and breaks) of less than 120 minutes.

2.5. Recording

MfVEPs were recorded from 3 gold cup electrodes referenced to the inion (Iz; Fig. 1B): electrodes were placed 4 cm left and right (OL and OR) as well as 1 cm above Iz, and at Oz (American Clinical Neurophysiology Society, 2006). The signal was amplified by 100 k with a physiological amplifier (Grass Model 12, Astro-Med, Inc., West Warwick, RI, USA), band-pass filtered (low and high frequency cut-offs: 3 and 100 Hz), and digitized at 1200 Hz.

2.6. Analysis

"The isolation of responses to pattern-reversal stimulation requires the extraction of the responses to the change of the visual stimulus from one m-sequence step to the other, i.e. a change from a 4-by-4 checkerboard pattern to its contrast-inverted variant. This was achieved by extracting the first slice of the second order kernel, as defined by (Sutter, 2000), for the recorded responses using VERIS 6.4.7X. All subsequent analyses were performed with custom made tools written in IGOR 6.22 (WaveMetrics Inc., Lake Oswego, OR, USA). Traces were digitally filtered (high pass cut-off: 3 Hz; low pass cut-off: 30 Hz)" (Herbik et al., 2014), which is in accordance with previously established procedures (Hood and Greenstein, 2003). For both experiments the traces for the two repetitions, obtained for each photopic and scotopic fixation condition, were averaged.

2.7. MfVEP analysis

Due to the cortical convolution there is generally a high degree of variability in the mfVEP trace shapes and polarities across the visual field and within and across individuals [reviewed in (Hood and Greenstein, 2003; Hoffmann, 2008)]. E.g., there is a systematical variation of trace shapes across the visual field for mfVEP responses recorded from Oz vs Iz (i.e., Channel 1 in Fig. 1B), i.e. the tendency for a polarity reversal of upper compared to lower hemifield responses which is caused by the cortical convolution comprising the calcarine sulcus. Response quantifications based on peak-to-peak measurements are therefore an unreliable approach and root-mean-squares are the preferred measure to quantify response magnitudes. To assess signal presence, we therefore determined the root-mean-square (RMS) of the mfVEP in a signal and a noise window for all 36 tested visual fields. The photopic signal time window (TW$_P$) spanned 45–150 ms and the noise window 325–430 ms, the scotopic signal time window (TW$_S$) and noise window were shifted by 96 ms (for both mfVEP$_{S-}$ and mfVEP$_{S+}$); this amount of shift was determined by finding the time window with the maximal SNR for the mfVEP$_S$ in a stepwise iterative process. With these RMS-values we computed the signal-to-noise ratio (SNR) of the mfVEP responses in each *i*-th sector (of the $n = 36$ total sectors) of participant *j* defined, for the TW$_P$, as

$$SNR_{ij} = RMS_{ij}(45 \text{ to } 150 \text{ ms})/[\sum_i RMS_{ij}(325 \text{ to } 430 \text{ ms})/n] \quad (1)$$

and for TW$_S$, as

$$SNR_{ij} = RMS_{ij}(141 \text{ to } 246 \text{ ms})/[\sum_i RMS_{ij}(421 \text{ to } 526 \text{ ms})/n] \quad (2)$$

To determine the SNR-values indicative of a significant mfVEP response, an estimate of the false positive rates was determined for the data of the present study with an assessment of the distribution of noise-SNR values, i.e. calculated for the noise window (Zhang et al., 2002) using Eq. (3) for the TW$_P$

$$SNR_{ij} = RMS_{ij}(325 \text{ to } 430 \text{ ms})/[\sum_i RMS_{ij}(325 \text{ to } 430 \text{ ms})/n] \quad (3)$$

and Eq. (4) for the TW$_s$

$$SNR_{ij} = RMS_{ij}(421 \text{ to } 526 \text{ ms})/[\sum_i RMS_{ij}(421 \text{ to } 526 \text{ ms})/n] \quad (4)$$

This analysis showed that SNR-values ≥2 are part of the noise distribution with a mean probability of 5%. Subsequently, this SNR threshold of 2 was applied to the mfVEP-SNR-values to exclude visual field locations without recordable signals from our analyses, i.e. those locations that failed to exceed an SNR threshold of 2 in any of the conditions of the respective experiment. This procedure is in accordance with previously established and commonly applied procedures (Zhang et al., 2002; Hood and Greenstein, 2003).

Following previous procedures (Hood et al., 2002) the 3 physical channels were used to calculate further 3 channels (Fig. 1B). Out of the resulting total of 6 channels that one with highest SNR for either condition (mfVEP$_P$ or mfVEP$_S$) was selected for further

analysis and to visualize the visual field topography of the cortical responses for each of the 36 visual field locations.

"For each participant the mfVEP response latency shifts (photopic vs scotopic) were determined by calculating the cross-correlation of the respective trace pairs. This analysis yielded the delay for each correlated trace pair (Hood et al., 2004). Specifically, the cross-correlations were calculated for the traces obtained for two different experimental conditions" (Herbik et al., 2014), i.e., photopic and scotopic, at the same visual field location and for the same derivation within a time-window of ±105 ms. "Only trace pairs with at least one trace with super-threshold SNR were included in the analysis, visual field locations with sub-threshold SNR in both traces were discarded (see above). The mean delay and standard deviation were calculated from these data" (Herbik et al., 2014).

2.8. Statistics

SNRs follow a normal distribution only after logarithmizing (Hood and Greenstein, 2003). Therefore SNRs were logarithmized

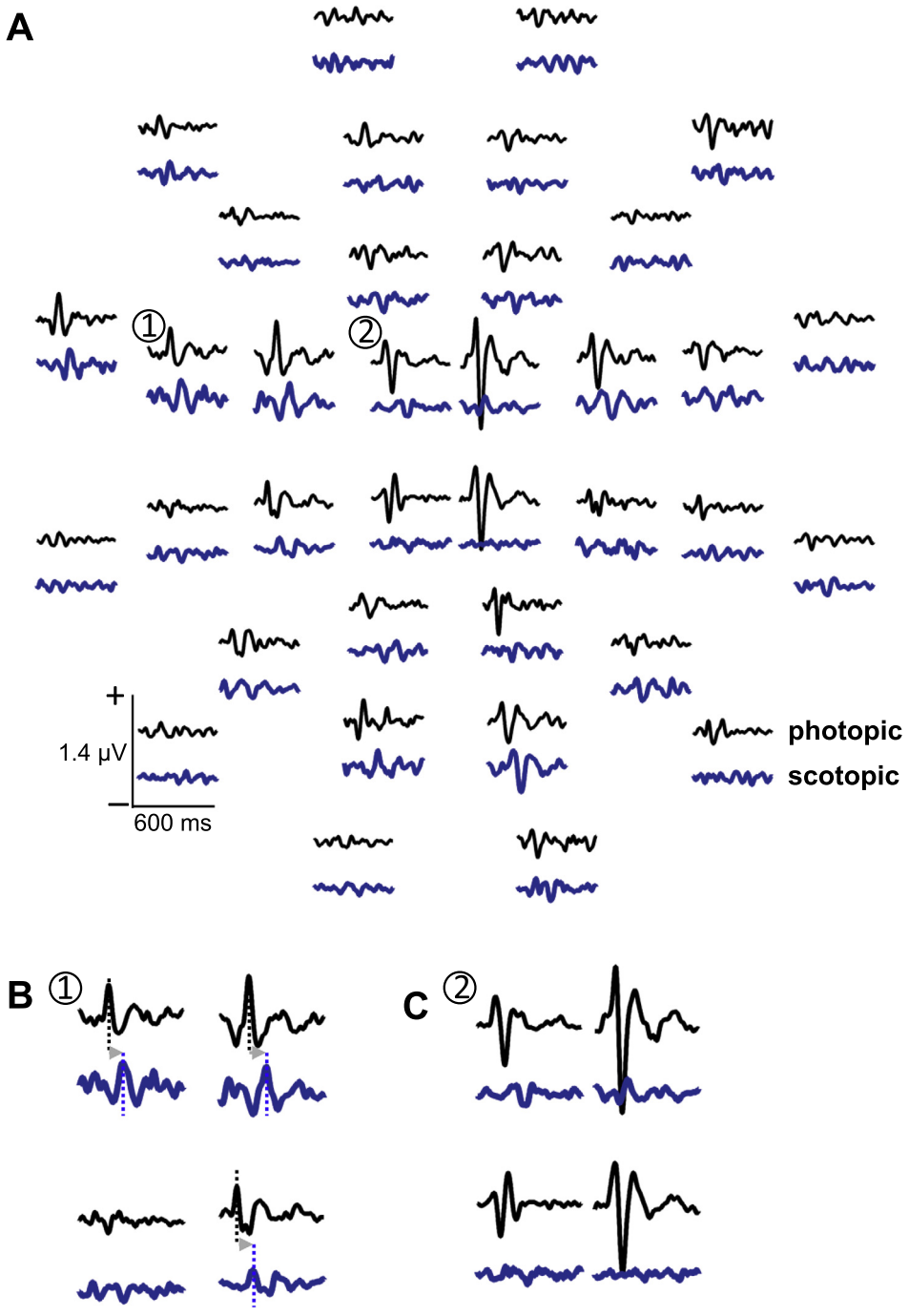

Fig. 2. mfVEP traces arrays (Experiment 1) for a representative participant for $mfVEP_P$ (black traces (upper rows)) and $mfVEP_{S-}$ (blue traces (lower rows); without additional fixation aid). (A) mfVEP are arranged as a back-projection to the visual field locations that evoked them. Note that the actual stimulus was scaled with eccentricity (Fig. 1), while the traces are equidistant. Traces were combined from the 6 channels (3 physical and 3 calculated, see Fig. 1 (B) as described in Methods. While $mfVEP_P$ and $mfVEP_{S-}$ have similar trace shapes, $mfVEP_{S-}$ are delayed (see magnified responses from left visual field in B) and reduced in the centre (see magnification in C).

for descriptive statistics and the assessment of the significance of effects. For depiction and assessment of the results de-logarithmized values are given. To assess whether $mfVEP_{S+}$ were decreased e.g. due to light adaptation, a two-way repeated measures ANOVA with the factors 'fixation aid' [$mfVEP_{S-}$ (experiment 1, fixation aid off) and $mfVEP_{S+}$ (experiment 2: fixation aid on)] and 'eccentricity' (4 eccentricities) was conducted using SPSS 24 (IBM, NY, USA) comparing the logarithmized mfVEP-SNR values.

3. Results

3.1. Comparison of photopic and scotopic mfVEP

Both scotopic and photopic responses, i.e. $mfVEP_P$ and $mfVEP_P$, reflect typical hallmarks of multifocal VEP recordings (see Supplementary Figs. 1 and 2). For a qualitative assessment the visual field topography of photopic and scotopic cortical responses, i.e. $mfVEP_P$

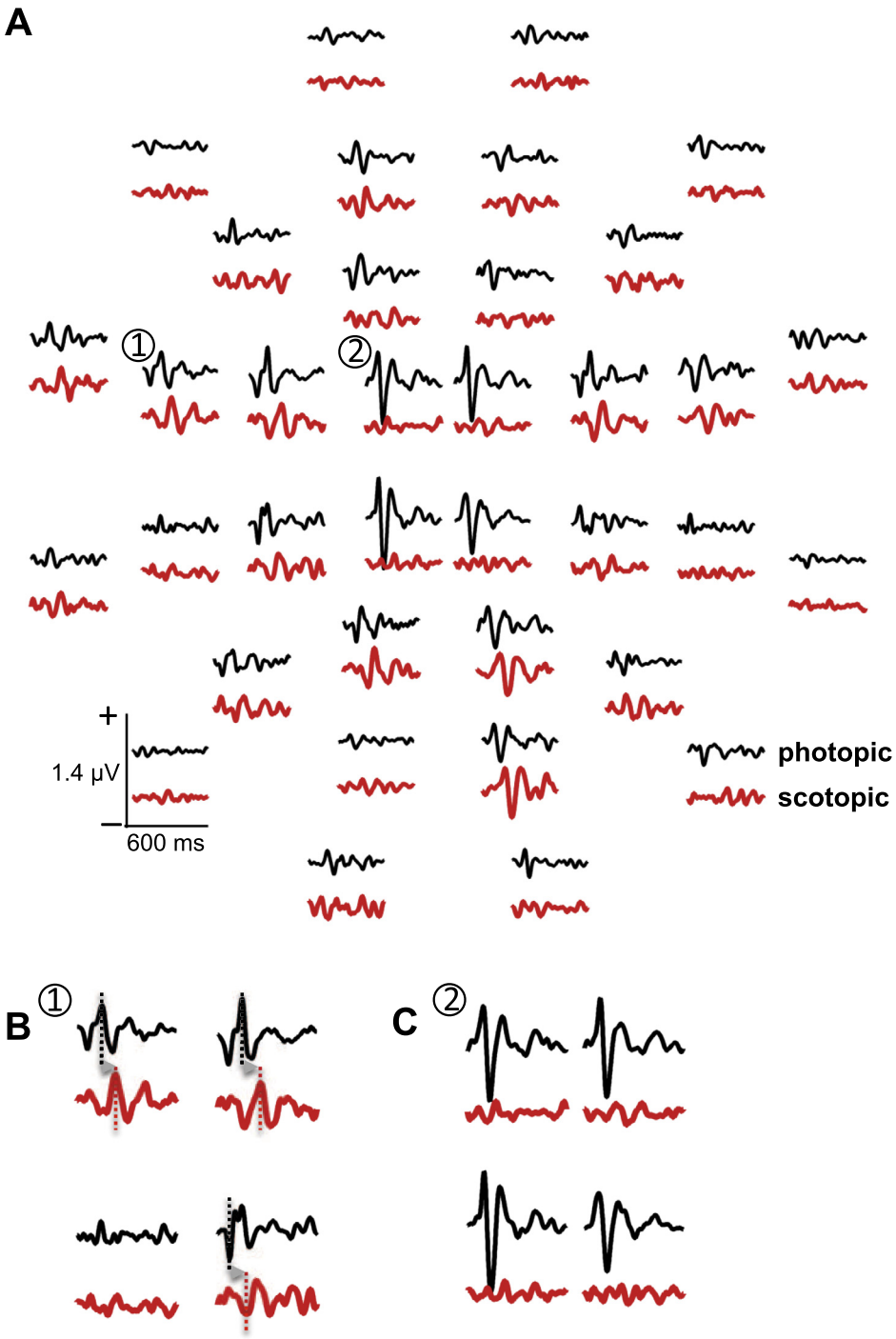

Fig. 3. mfVEP traces arrays (Experiment 2) for the same participant as in Fig. 2 for $mfVEP_P$ (black traces (upper rows)) and $mfVEP_{S+}$ (red traces (lower rows); with additional fixation aid). Conventions as in Fig. 2A–C. While $mfVEP_P$ and $mfVEP_{S+}$ have similar trace shapes, $mfVEP_{S+}$ are delayed (see magnified responses from left visual field in B) and in the center reduced (see magnification in C).

and $mfVEP_S$, are depicted for a representative participant in Fig. 2A (without additional fixation aid: $mfVEP_{S\_}$) and Fig. 3A (with additional fixation aid: $mfVEP_{S+}$; respective data for a second participant are given in Supplementary Fig. 3) as derived from the combined multichannel recording (see Methods). Typical $mfVEP_P$ were obtained, i.e. greatest response magnitudes in the central visual field and a decrease of response magnitudes towards the periphery. In contrast, both $mfVEP_{S\_}$ and $mfVEP_{S+}$, response magnitudes were severely reduced for central visual field locations (see Figs. 2C and 3C). Further, for para- and extracentral visual field locations sizable mfVEP responses were evident for both photopic and scotopic conditions, however, with a delay for the $mfVEP_S$ as indicated by the trace shift of both $mfVEP_{S\_}$ and $mfVEP_{S+}$ highlighted in Fig. 2B and 3B and Supplementary Fig. 3.

Supplementary data associated with this article can be found, in the online version, at https://doi.org/10.1016/j.clinph.2018.11.030.

For a quantitative comparison of the mfVEP-response timing during photopic and scotopic conditions, cross-correlations were performed between $mfVEP_P$ and $mfVEP_S$ for each participant as detailed in Methods, to determine the median delays of the scotopic responses. Compared to $mfVEP_P$, $mfVEP_{S\_}$ (Experiment 1, i.e. without fixation aid) were delayed by a median of 100.8 ms [lower quartile: 97.5 ms; upper quartile: 108.3 ms] and $mfVEP_{S+}$ (Experiment 2, i.e. with fixation aid) were delayed by 96.7 ms [lower quartile 95.8 ms; upper quartile 99.2 ms].

For a quantitative comparison of the mfVEP-response magnitudes, SNR-values were determined for $mfVEP_P$ and $mfVEP_S$ for a scotopic and photopic time-window as detailed in Methods. This way the response shift between photopic and scotopic responses was taken into account for the analysis of the respective response magnitudes. The eccentricity dependence of the SNRs for $mfVEP_P$ and $mfVEP_S$ is given in Fig. 4. $MfVEP_P$ SNRs follow the expected eccentricity dependence, i.e. biggest responses in the center (SNR = 16.2) and a gradual response reduction toward the periphery, down to an SNR of 3.4. $MfVEP_S$ SNRs fall short of that for the $mfVEP_P$ for all eccentricities. Moreover, they differ in their eccentricity dependence, i.e. the central SNRs [0°–4°] are smallest for $mfVEP_{S\_}$, i.e., 1.7 ± 0.11, and $mfVEP_{S+}$, i.e., 1.8 ± 0.08 (SEM), and thus fall short of the SNR threshold of 2.0 (determined as described in Methods); extracentral SNRs are 2.4 (SEM: −0.2 and +0.3) and 2.8 ± 0.2 [4°–9°], 2.5 ± 0.2 and 3.1 ± 0.2 [9°–16°], 2.0 ± 0.1 and 2.2 ± 0.1 [16°–25°], for $mfVEP_{S\_}$ and $mfVEP_{S+}$, respectively.

3.2. Effects of an additional fixation aid

To test whether the additional fixation aid might reduce peripheral amplitudes, e.g., via stray-light induced luminance adaptation, we applied a two-factor repeated measures ANOVA (factors 1: fixation aid; factor 2: and eccentricity) to the $mfVEP_S$ SNRs. Neither of the two factors, nor their interaction did show a significant effect on the response magnitudes. If any effect, there was a trend for increased amplitudes for extracentral $mfVEP_{S+}$ (by on average 19% logarithmized SNR), which just missed the 5% significance threshold ($p < 0.058$). As we had a small sample size ($n = 9$), we assessed the statistical power of our approach with sequentially Bonferroni-corrected paired t-tests (Holm, 1979). These indicated that changes in logarithmized SNR below 20% (eccentricity ranges 4°–9° and 16°–25°) remain undetected for our sample size, while a 22% change appeared detectable (eccentricity ranges 9°–16°). This suggests that instead of a response reduction there might be a response increase for $mfVEP_{S+}$, which, on average, falls short of 20%. In conclusion, no indication of a response reduction of extracentral amplitudes was detected for the condition with an additional fixation aid ($mfVEP_{S+}$).

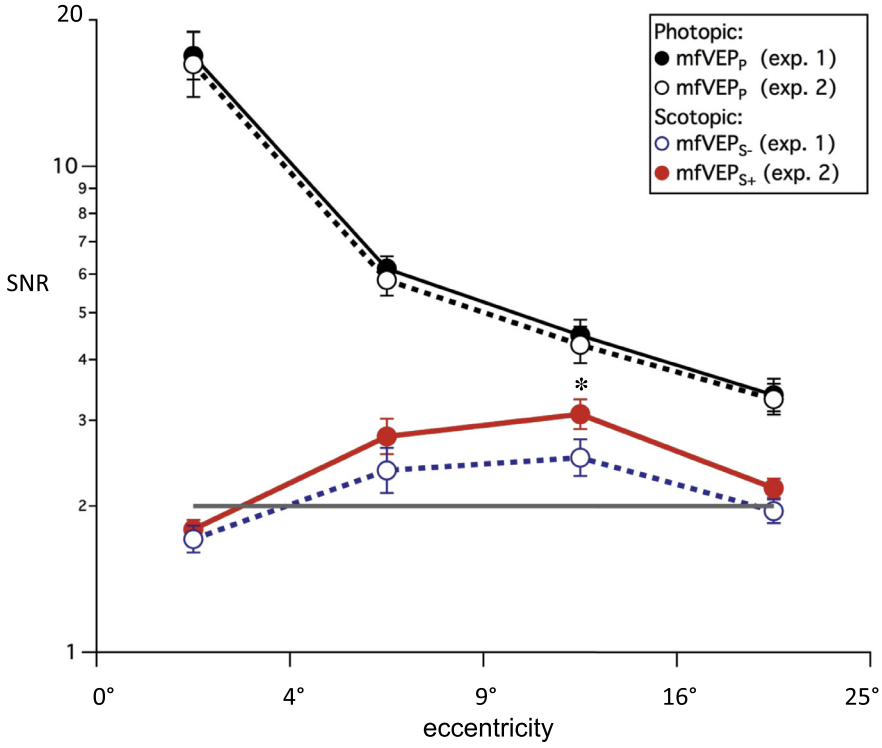

Fig. 4. mfVEP SNR (mean ± SEM; n = 9) analyses averaged across participants in an eccentricity dependent manner for Experiment 1 (dashed lines) and Experiment 2 (solid lines). Conditions are identical for both $mfVEP_P$ recordings thus underlining the reproducibility. Overall $mfVEP_S$ SNRs (top traces) generally fall short of the $mfVEP_P$ SNRs (bottom traces). Both $mfVEP_{S\_}$-SNR and $mfVEP_{S+}$-SNR in the center [0°–4°] are below the SNR-threshold of 2.0.

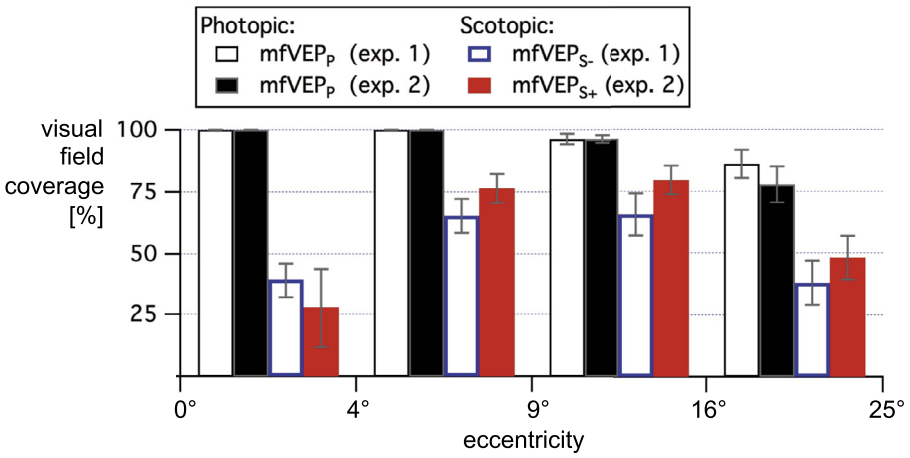

Fig. 5. Average visual field coverage based on photopic (left bar pairs) and scotopic mfVEP (right bar pairs) measurements (mean ± SEM; n = 9). Percentage of visual field locations with super-threshold SNR is given as a function of eccentricity.

3.3. Visual field coverage

Photopic mfVEP can be used for objective visual field assessments as responses can be obtained from most visual field locations, i.e. mfVEP provide high visual field coverage. To assess the potential of scotopic mfVEP for objective scotopic perimetry, we here compared the visual field coverage of photopic and scotopic measurements. We determined the percentage of responsive locations, i.e. with superthreshold SNR (SNR > 2.0), in an eccentricity dependent manner for mfVEP$_P$, mfVEP$_{S+}$, and mfVEP$_{S-}$(Fig. 5). For the photopic condition, i.e. mfVEP$_P$, for both Experiments there was as expected a similarly high visual field coverage: 100% [0°–4°], 100% [4°–9°], 96% [9°–16°], and 86% and 77% [16°–25°] for Experiment 1 and Experiment 2, respectively. For the scotopic condition, i.e. mfVEP$_{S+}$ and mfVEP$_{S-}$, visual field coverage was 27.8% and 38.8% [0°–4°], 76.4% and 65.3% [4°–9°], 79.6% and 65.7% [9–16°], 48.1% and 37% [16°–25°], respectively.

4. Discussion

Pioneering the objective spatially resolved assessment of scotopic vision, we recorded mfVEP$_S$ at stimulus mean luminance of 0.003 cd/m^2 and tested whether the responses reflected typical features of scotopic vision, reduced central and delayed extracentral responses. Further, we explored the effect of an additional fixation aid to support central fixation (mfVEP$_{S+}$ as opposed to mfVEP$_{S-}$). Compared to photopic mfVEP$_P$, responses were reduced below SNR-threshold in the center (0°–4°), independent of the fixation condition, and superthreshold beyond the center, where we observed delays of on average 101 ms (mfVEP$_{S-}$) and 97 ms (mfVEP$_{S+}$). Consequently, the hallmarks of scotopic vision were evident independent of the specific fixation condition.

Similar effects to those reported in the present study for mfVEP have previously been reported for conventional VEP (cVEP) recorded under scotopic and photopic conditions (Kubová et al., 2004; Rudvin and Valberg, 2006). Specifically, scotopic compared to photopic cVEPs to pattern-reversal and flash stimulation were, as for the obtained mfVEP$_S$, reduced in magnitude compared to photopic cVEPs. They were also reported to be delayed relative to photopic cVEPs by around 140 ms [Kubová et al. (2004), pattern-reversal cVEP] and 90 ms (Rudvin and Valberg, 2006) for similar photopic and scotopic luminances as for the present study. This delay is in the same order as the shift reported here for the mfVEP$_S$, i.e. on average 101 ms (mfVEP$_{S-}$) and 97 ms (mfVEP$_{S+}$).

4.1. Features of scotopic vision to characteristics of mfVEPS

The rod-free area of the fovea corresponds to a visual field region of 1.25° diameter (Curcio et al., 1990). The central scotoma during scotopic vision exceeds this size, due to the scarcity of parafoveal rods, and ranges between around 2° to 4° diameter (Barton and Brewer, 2015; Baseler et al., 2002; Hadjikhani and Tootell, 2000; Hubel et al., 2009). In fact, progressing from the fovea, rod density increases at first gradually and eventually peaks beyond 15° (Osterberg, 1935). As a consequence, we here found mfVEP$_S$ for the central 8° diameter to be reduced down to noise levels, which corresponds to reduced central and paracentral rod densities. Unexpectedly, however, small mfVEP$_S$-SNRs were also obtained for the largest eccentricities stimulated, i.e. 16°–25°. While this appears at first sight counterintuitive, it should be noted that the spatial resolution for scotopic vision in general falls short of that for photopic vision (Hecht and Mintz, 1939; D'Zmura and Lennie, 1986; Benedek et al., 2003). Consequently, the pattern-sizes of the circular checkerboard used for the mfVEP-recordings might elicit stronger responses for the photopic compared to the scotopic condition, due to the mismatch of scotopic spatial retinal sampling and stimulus grain. We assume that this mismatch was evident for the peripheral stimuli. Optimising stimulus dimensions for scotopic recording conditions appears therefore to be a rewarding strategy to increase mfVEP$_S$ amplitudes in follow-up studies.

4.2. Practical considerations

The present study provides important insights into and an initial proof-of-concept of scotopic mfVEP in 9 participants with normal vision. The technique may hold the promise of an objective, spatially resolved visual field test and motivates testing the approach in patients with diseases affecting scotopic vision. For the translation of the approach into research and clinics, however, potential confounds such as fixation inaccuracy and small SNRs will have to be addressed in order to provide an objective quantitative account of scotopic visual function across the visual field.

Clearly, compromised central fixation is a potential confound for visual system investigations during scotopic conditions. Due to the central dark scotoma, there is a tendency for the fixation

to be shifted into the upper right hemifield (Aulhorn and Michelfelder, 1972). This eccentric fixation can be counteracted by different measures. E.g., by presenting a large fixation cross and instructing the observers to place their central scotoma such that it covers the crossing point of the lines. In addition, a mesopic central long wavelength fixation target can be presented to stimulate the foveal cones and thus support foveal fixation. Care, however, must be taken, to check whether such an additional non-scotopic stimulus degrades dark-adaptation beyond the fovea and therefore reduce parafoveal and peripheral responses. We therefore compared $mfVEP_S$ for both strategies to reduce confound of fixation inaccuracies. In fact, we observed no amplitude decrease, if any, there was a trend for an amplitude increase of extracentral responses for the additional fixation target. We therefore conclude, that the use of an additional mesopic fixation target supports fixation stability and hence increases response-SNRs and the accuracy of scotopic mfVEP-recordings. Therefore the $mfVEP_{S+}$ condition is preferable to the $mfVEP_{S-}$ condition for a spatially resolved scotopic visual function assessment. Ultimately, of course, fundus-controlled, ideally fundus-stabilized, stimulation would be of benefit to determine and eventually eliminate the effects of fixation instabilities on the recordings. As fixation jitter reduces multifocal response amplitudes (Chisholm et al., 2001; Rudolph and Kalpadakis, 2002; Menz et al., 2004; Hoffmann and Seufert, 2005; Hoffmann et al., 2006; Zhang et al., 2008), this would also help to increase $mfVEP_S$ magnitudes and hence SNRs to optimize the visual field coverage for mfVEP-based objective visual field testing.

For an objective visual field test, false negative responses, i.e., spurious scotomas, are, as a matter of course, a strong confound. We assessed the visual field coverage of $mfVEP_P$ and $mfVEP_S$ and observed full visual field coverage for $mfVEP_P$ with a slight drop off in the periphery. In contrast, for $mfVEP_{S+}$ the coverage exceeded 75% only for two eccentricity bins, those spanning 4°–9° and 9°–16°. There is a potential to increase the specificity of the detection of scotomas by adding additional criteria as previously applied to $mfVEP_P$, such as the contingency of mfVEP-dropouts (Hood and Greenstein, 2003), but that would, as a matter of course, be at the expense of sensitivity and spatial resolution. Taken together, for the present settings the $mfVEP_{S+}$, allows only for 'crude' objective scotopic visual field testing in an eccentricity range from 4° to 16°. This prompts the question, of how the visual field coverage can be increased for this eccentricity range and beyond. A key is to increase $mfVEP_S$ SNRs, e.g by the means already suggested above: (i) Fundus-stabilized recording would not only increase spatial specificity, but also SNRs; (ii) applying a spatial stimulus layout that guarantees a closer match between the scotopic retinal sampling and the spatial frequency of the applied stimulus, is expected to increase $mfVEP_S$ SNRs. While both approaches are challenging and require further investigations, they appear rewarding as objective scotopic visual field testing is of value for both clinical research and diagnostics.

In conclusion, we provide important insights into and an initial proof-of-concept of scotopic mfVEP in our 9 normal volunteer subjects, which motivate the testing of patients with poor scotopic vision in follow-up studies. Further, we indicate routes to overcome current limitations to pursue future applications in research and clinics such that the technique may hold the promise of an objective, spatially resolved visual field test for patients with diseases affecting scotopic vision.

Acknowledgements

The support by the DFG (HO2002/12-1) is gratefully acknowledged.

Conflict of Interest Statement

None.

References

American Clinical Neurophysiology Society. Guideline 5: Guidelines for standard electrode position nomenclature. J Clin Neurophysiol 2006;23:107–10.
Aulhorn E, Michelfelder F. Comparison of fixation displacement in organic macula diseases and in physiologic dark scotoma. Ber Uber Zusammenkunft Dtsch Ophthalmol Ges 1972;71:487–91.
Bach M, Kellner U. Elektrophysiologische Diagnostik in der Ophthalmologie. Ophthalmol 2000;97:898–920.
Barton B, Brewer AA. fMRI of the rod scotoma elucidates cortical rod pathways and implications for lesion measurements. Proc Natl Acad Sci 2015;112:5201–6.
Baseler HA, Brewer AA, Sharpe LT, Morland AB, Jägle H, Wandell BA. Reorganization of human cortical maps caused by inherited photoreceptor abnormalities. Nat Neurosci 2002;5:364–70.
Benedek G, Benedek K, Kéri S, Letoha T, Janáky M. Human scotopic spatiotemporal sensitivity: a comparison of psychophysical and electrophysiological data. Doc Ophthalmol Adv Ophthalmol 2003;106:201–7.
Chen C, Wu L, Wu D, Huang S, Wen F, Luo G, et al. The local cone and rod system function in early age-related macular degeneration. Doc Ophthalmol Adv Ophthalmol 2004;109:1–8.
Chisholm JA, Keating D, Parks S, Evans AL. The impact of fixation on the multifocal electroretinogram. Doc Ophthalmol Adv Ophthalmol 2001;102:131–9.
Cohn M, Lempel A. On fast M-sequence transforms (Corresp.). IEEE Trans Inf Theory. 1977;23:135–7.
Curcio CA, Sloan KR, Kalina RE, Hendrickson AE. Human photoreceptor topography. J Comp Neurol 1990;292:497–523.
D'Zmura M, Lennie P. Shared pathways for rod and cone vision. Vision Res 1986;26:1273–80.
Feigl B, Brown B, Lovie-Kitchin J, Swann P. Cone- and rod-mediated multifocal electroretinogram in early age-related maculopathy. Eye Lond Engl 2005;19:431–41.
Feigl B, Brown B, Lovie-Kitchin J, Swann P. The rod-mediated multifocal electroretinogram in aging and in early age-related maculopathy. Curr Eye Res 2006;31:635–44.
Hadjikhani N, Tootell RB. Projection of rods and cones within human visual cortex. Hum Brain Mapp 2000;9:55–63.
Hecht S, Mintz EU. The visibility of single lines at various illuminations and the retinal basis of visual resolution. J Gen Physiol 1939;22:593–612.
Hecht S, Shlaer S. Intermittent stimulation By light: V. The relation between intensity and critical frequency for different parts of the spectrum. J Gen Physiol 1936;19:965–77.
Heckenlively J, Arden G. Principles and practice of clinical electrophysiology of vision, 2nd Edition. MIT CogNet; 2006 [cited 2018 Jul 20]. Available from: http://cognet.mit.edu/erefs/principles-and-practice-of-clinical-electrophysiology-of-vision-2nd-edition.
Herbik A, Reupsch J, Thieme H, Hoffmann MB. Differential effects of optic media opacities on simultaneous multifocal pattern electroretinograms and visual evoked potentials. Clin Neurophysiol 2014;125:2418–26.
Hoffmann MB. Investigating visual function with multifocal visual evoked potentials [cited 2018 Jul 20]. In: Lorenz B, Borruat FX, editors. Pediatric ophthalmology, neuro-ophthalmology, genetics. Essentials in ophthalmology. Berlin, Heidelberg: Springer; 2008. p. 139–59.
Hoffmann MB, Flechner J-J. Slow pattern-reversal stimulation facilitates the assessment of retinal function with multifocal recordings. Clin Neurophysiol 2008;119:409–17.
Hoffmann MB, Heinrich SP, Thieme H, Al-Nosairy KO. Reaching Beyond the Retina with Clinical Electrophysiology. Klin Monbl Augenheilkd 2018;235:1229–34.
Hoffmann MB, Lorenz B, Preising M, Seufert PS. Assessment of cortical visual field representations with multifocal VEPs in control subjects, patients with albinism, and female carriers of ocular albinism. Invest Ophthalmol Vis Sci 2006;47:3195–201.
Hoffmann MB, Seufert PS. Simulated nystagmus reduces pattern-reversal more strongly than pattern-onset multifocal visual evoked potentials. Clin Neurophysiol 2005;116:1723–32.
Hoffmann MB, Straube S, Bach M. Pattern-onset stimulation boosts central multifocal VEP responses. J Vis 2003;3:432–9.
Hoffmann MB, Thieme H, Liedecke K, Meltendorf S, Zenker M, Wieland I. Visual pathways in humans with Ephrin-B1 deficiency associated with the cranio-fronto-nasal syndrome. Invest Ophthalmol Vis Sci 2015;56:7427–37.
Hoffmann MB, Wolynski B, Bach M, Meltendorf S, Behrens-Baumann W, Golla F. Optic nerve projections in patients with primary ciliary dyskinesia. Invest Ophthalmol Vis Sci 2011;52:4617–25.
Holm S. A simple sequentially rejective multiple test procedure. Scand J Stat 1979;6:65–70.
Hood DC, Greenstein VC. Multifocal VEP and ganglion cell damage: applications and limitations for the study of glaucoma. Prog Retin Eye Res 2003;22:201–51.
Hood DC, Ohri N, Yang EB, Rodarte C, Zhang X, Fortune B, et al. Determining abnormal latencies of multifocal visual evoked potentials: a monocular analysis. Doc Ophthalmol 2004;109:189–99.

Hood DC, Wladis EJ, Shady S, Holopigian K, Li J, Seiple W. Multifocal rod electroretinograms. Invest Ophthalmol Vis Sci 1998;39:1152–62.
Hood DC, Zhang X, Hong JE, Chen CS. Quantifying the benefits of additional channels of multifocal VEP recording. Doc Ophthalmol 2002;104:303–20.
Hubel DH, Howe PDL, Duffy AM, Hernández A. Scotopic foveal afterimages. Perception 2009;38:313–6.
Kubová Z, Kremlácek J, Kuba M, Chlubnová J, Sverák J. Photopic and scotopic VEPs in patients with congenital stationary night-blindness. Doc Ophthalmol Adv Ophthalmol 2004;109:9–15.
MacLeod DI. Rods cancel cones in flicker. Nature 1972;235:173–4.
Markó K, Mikó-Baráth E, Kiss HJ, Török B, Jandó G. Effects of luminance on dynamic random-dot correlogram evoked visual potentials. Perception 2012;41:648–60.
Menz M, Sutter E, Menz M. The effect of fixation instability on the multifocal VEP. Doc Ophthalmol 2004;109:147–56.
Odom JV, Bach M, Brigell M, Holder GE, McCulloch DL, Mizota A, et al. ISCEV standard for clinical visual evoked potentials: (2016 update). Doc Ophthalmol Adv Ophthalmol 2016;133:1–9.
Osterberg G. Topography of the layer of rods and cones in the human retina. Acta Ophthalmol Suppl 1935;6:1–103.
Rudolph G, Kalpadakis P. The role of fixation for reliable mfERG results. Graefes Arch Clin Exp Ophthalmol 2002;240:874–5. author reply 876-877.
Rudvin I, Valberg A. Flicker VEPs reflecting multiple rod and cone pathways. Vision Res 2006;46:699–717.
Sutter E. Multi-input VER and ERG analysis for objective perimetry. In: IEEE7th Annu Conf Eng Med Biol Soc 1985; 1985: p. 415–9.
Sutter E. The fast m-transform: a fast computation of cross-correlations with binary m-sequences. SIAM J Comput 1991;20:686–94.
Sutter E. The interpretation of multifocal binary kernels. Doc Ophthalmol Adv Ophthalmol 2000;100:49–75.
Zele AJ, Cao D. Vision under mesopic and scotopic illumination. Front Psychol 2014;5:1594.
Zhang B, Stevenson SS, Cheng H, Laron M, Kumar G, Tong J, et al. Effects of fixation instability on multifocal VEP (mfVEP) responses in amblyopes. J Vis. 2008;8. 16 16.
Zhang X, Hood DC, Chen CS, Hong JE. A signal-to-noise analysis of multifocal VEP responses: an objective definition for poor records. Doc Ophthalmol 2002;104:287–302.